Clim Dyn (2016) 46:291–302
DOI 10.1007/s00382-015-2584-3

# Southern Tibetan Plateau ice core $\delta^{18}O$ reflects abrupt shifts in atmospheric circulation in the late 1970s

**Jing Gao[1,2] · Camille Risi[3] · Valerie Masson-Delmotte[4] · You He[1,5] · Baiqing Xu[1,2]**

Received: 25 June 2014 / Accepted: 29 March 2015 / Published online: 16 April 2015


**Abstract** Ice cores from the Tibetan Plateau provide high-resolution records of changes in the snow and ice isotopic composition. In the monsoon sector of southern Tibetan Plateau, their climatic interpretation has been controversial. Here, we present a new high-resolution $\delta^{18}O$ record obtained from 2206 measurements performed at 2–3 cm depth resolution along a 55.1 m depth ice core retrieved from the Noijinkansang glacier (NK, 5950 m a.s.l.) that spans the period from 1864 to 2006 AD. The data are characterized by high $\delta^{18}O$ values in the nineteenth century, 1910s and 1960s, followed by a drop in the late 1970s and a recent increasing trend. The comparison with regional meteorological data and with a simulation performed with the LMDZiso general circulation model leads to the attribution of the abrupt shift in the late 1970s predominantly to changes in regional atmospheric circulation, together with the impact of atmospheric temperature change. Correlation analyses suggest that the large-scale modes of variability (PDO and ENSO, i.e. Pacific Decadal Oscillation and El Nino-Southern Oscillation) play important roles in modulating NK $\delta^{18}O$ changes. The NK $\delta^{18}O$ minimum at the end of the 1970s coincides with a PDO phase shift, an inflexion point of the zonal index (representing the overall intensity of the surface westerly anomalies over middle latitudes) as well as ENSO, implying interdecadal modulation of the influence of the PDO/ENSO on the Indian monsoon on southern TP precipitation $\delta^{18}O$. While convective activity above North India controls the intra-seasonal variability of precipitation $\delta^{18}O$ in southern TP, other processes associated with changes in large-scale atmospheric circulation act at the inter-annual scale.

**Keywords** Ice core $\delta^{18}O$ · Large-scale atmospheric circulation · Isotopic general circulation model · Southern Tibetan Plateau

## 1 Introduction

The Tibetan Plateau (TP) is a unique area where the topography plays a key role in the regional atmospheric circulation and the hydrological cycle, which encompasses the largest number of glaciers outside of polar regions (Yao et al. 2012). Short instrumental records from inhabited areas depict a recent large warming trend (Liu and Chen 2000; Wang et al. 2008; Qin et al. 2009). Natural archives allow us to place recent changes in the broader context of natural climate variability. Among them, ice cores provide high-resolution proxy records of climate variability, archived through e.g. changes in water stable isotopes (usually expressed in a delta notation, such as $\delta^{18}O$ used hereafter). However, their climatic interpretation requires us to

**Electronic supplementary material** The online version of this article (doi:10.1007/s00382-015-2584-3) contains supplementary material, which is available to authorized users.

✉ Jing Gao
gaojing@itpcas.ac.cn

1 Key Laboratory of Tibetan Environment Changes and Land Surface Processes, Institute of Tibetan Plateau Research, Chinese Academy of Sciences, Beijing, China

2 CAS Center for Excellence in Tibetan Plateau Earth Sciences, Beijing 100101, China

3 LMD/IPSL, CNRS, UPMC, Paris, France

4 LSCE, UMR 8212 CEA/CNRS/UVSQ – IPSL, Gif-sur-Yvette, France

5 State Key Laboratory of Cryospheric Sciences, Cold and Arid Regions Environment and Engineering Research Institute, Chinese Academy Sciences, Beijing, China

decipher the climatic controls on high-altitude precipitation $\delta^{18}O$. While northern TP $\delta^{18}O$ is mostly controlled by temperature-driven distillation, as in mid and high latitudes, the situation is more complex in the monsoon sector of the southern TP (Yao et al. 2013).

A number of studies have attributed recent increasing trends in south TP ice core $\delta^{18}O$ to regional warming (Thompson et al. 2000; Yao et al. 2006a; Zhao et al. 2012), while process-based studies have stressed the importance of changes in precipitation amount and Indian monsoon intensity (Vuille et al. 2005; Kaspari et al. 2007; Joswiak et al. 2010). Some authors have also stressed that spatial patterns are related to changes in air mass trajectories and moisture sources (Tian et al. 2003; Johnson and Ingram 2004; Breitenbach et al. 2010).

The southern TP climate is characterized by strong seasonal shifts in atmospheric circulation, as winter air masses are advected by the westerlies while summer atmospheric circulation is dominated by the Indian monsoon (Fig. 1a). Large-scale circulation indeed plays a key role in the spatial and seasonal distribution of southern TP precipitation $\delta^{18}O$ at intra-annual scales (Tian et al. 2001; Gao et al. 2011; Yao et al. 2013). Several studies have therefore suggested that TP ice cores record past variations of the regional atmospheric circulation (Qin et al. 2000; Kang et al. 2002, 2007b) which transports moisture from different sources (Tian et al. 2006), as also proposed for other locations (Meeker and Mayewski 2002; Kreutz et al. 2000; Hoffmann et al. 2003b; Xiao et al. 2004). So far, the exact processes relating atmospheric circulation and southern TP $\delta^{18}O$ have not been precisely identified and quantified.

Here, we present a new high-resolution isotopic record from an ice core recently drilled on the Noijinkansang (NK) glacier, southwest of Lhasa, which covers 2.7 $km^2$ in the southern TP (Fig. 1a) and extends from 5540 to 6674 m a.s.l.. During May 2007, our ice core was drilled to bedrock (55.1 m depth) at 5950 m a.s.l. in a flat basin of the accumulation zone of the NK glacier (29°2′8.68″N, 90°11′54.10″E, Fig. 1a). The nearest meteorological stations, Nagarze (29.96°N, 90.33°E, 4430 m a.s.l.) and Lhasa (29.70°N, 91.13°E, 3650 m a.s.l.), show that more than 80 % of annual precipitation occurs during the summer Indian monsoon season (June–September, hereafter JJAS, Fig. 1b), with a large inter-annual variability (Gao et al. 2009; Tian et al. 2001) (Fig. 1b). Monthly precipitation $\delta^{18}O$ from these stations displays a clear seasonal cycle, typical of southern TP, with maximum values in spring and minimum values in summer (Fig. 1b, Gao et al. 2009, 2013; Yao et al. 2013). This seasonal pattern is identified in the NK ice core and provides the basis for its age scale (Sect. 2).

This paper focuses on the climatic interpretation of the NK ice core $\delta^{18}O$ record (hereafter NK $\delta^{18}O$). In Sect. 3, we explore the statistical relationships between inter-annual $\delta^{18}O$ variations and local or regional temperature and precipitation data. Large-scale atmospheric teleconnections with NK $\delta^{18}O$ are also investigated. Atmospheric reanalyses, climate indices and an atmospheric general circulation model (LMDZiso) are used to identify and quantify the role of changes in large-scale atmospheric circulation on NK $\delta^{18}O$. Section 4 reports our conclusions and perspectives.

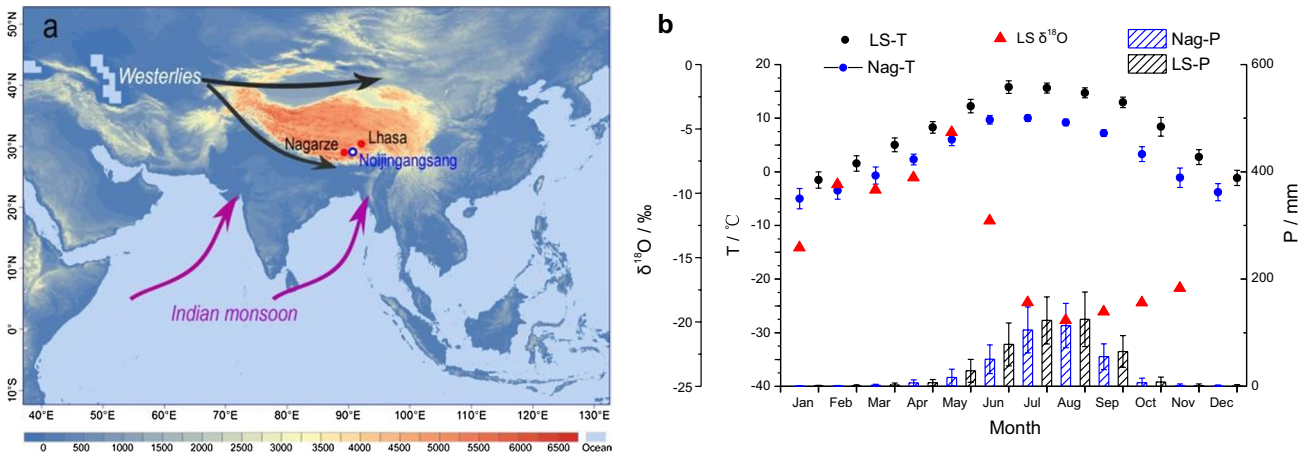


**Fig. 1** **a** General patterns of moisture transport towards the TP (*purple*, summer Indian monsoon; *black*, winter westerlies). The *blue circle* indicates the location of the ice core drilling site Noijingangsang. The position of the nearest meteorological stations (Lhasa and Nagarze) is shown by the *red filled circles*. **b** Mean seasonal cycle (1961–2006) of surface air temperature (T, °C, *circles*), precipitation amount (P, mm per month, *vertical bars*) at Lhasa (LS) and Nagarze (LKZ) meteorological stations, and monthly weighted precipitation $\delta^{18}O$ (‰, 1994–2006, triangles) at Lhasa. *Error bars* show the inter-annual standard deviation of air temperature and precipitation amount

## 2 Data

The NK ice core was cut into 2206 samples with intervals of 2 or 3-cm for analyses of stable isotopes, major soluble ions and carbonaceous aerosols, and 55 samples (~1 m resolution) for total beta radioactivity (hereafter β-activity) measurements. All the samples were transported to laboratory in frozen condition and melted at room temperature prior to analyses. Oxygen isotopes were measured using a MAT-253 mass spectrometer (with an analytical precision of 0.05 ‰) at the Key Laboratory of CAS for Tibetan Environment and Land Surface Processes, China. The β-activity was measured at the Analytical Laboratory of the Beijing Research Institute of Uranium Geology, China. The ice core is drilled on a vast and flat platform in the accumulation zone of the glacier, close to the ice divide. Field observations report no sign of surface wind mixing. Zhao et al. (2012) describes in details the ice core drilling and analytical procedures.

Below 16 m depth, the ice core density gradually increases to 0.9 g/cm$^3$, with no indication of melt or stratigraphic perturbation. The chronology is based on the identification of seasonal cycles in $\delta^{18}O$ and major soluble ions and verified using β-activity. The seasonal cycle of precipitation $\delta^{18}O$ is used to identify annual layers from one maximum of ice core $\delta^{18}O$ to the next one, therefore from spring (April–May) of 1 year to spring of the next year. The mean accumulation rate of the NK ice core of 470 mm w.e. is larger than the climatological precipitation amount at Lhasa and Nagarze (441.3 and 359.3 mm, respectively). Peaks in β-activity are detected at ~13.73 m (1987 Chernobyl event) and ~23.59 m (1963 nuclear bomb testing). The 55.1 m ice core is estimated to span 142 years (Fig. 2c). From repeated

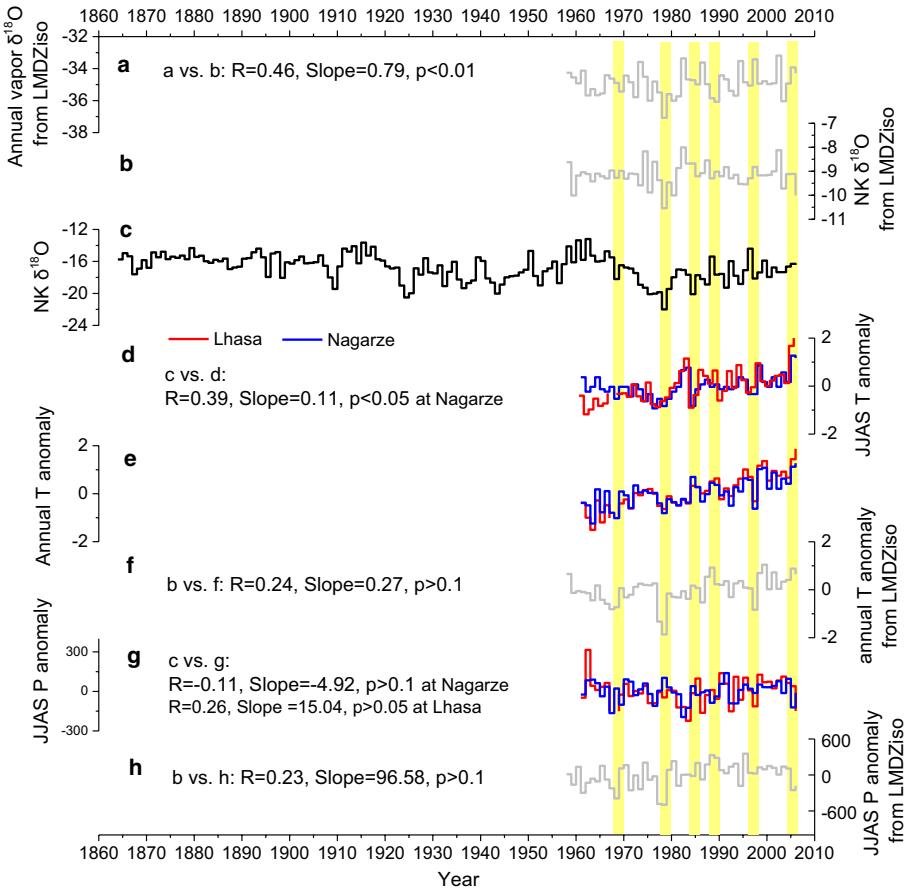


**Fig. 2** (*a*) Inter-annual variation of simulated JJAS vapor $\delta^{18}O$ anomaly from LMDZiso at the NK ice core site since 1958. (*b*) NK $\delta^{18}O$ from LMDZiso simulated in the corresponding region from 1958 to 2006. Inter-annual variations of (*c*) Noijinkansang ice core $\delta^{18}O$ from 1864 to 2006 compared with (*d*) JJAS temperature anomaly at Nagarze and Lhasa from 1961 to 2006, (*e*) annual temperature anomaly at Nagarze and Lhasa from 1961 to 2006, (*f*) simulated annual temperature anomaly from LMDZiso at the NK ice core site since 1958, (*g*) JJAS precipitation anomaly at Nagarze and Lhasa from 1961 to 2006, (*h*) simulated annual precipitation amount anomaly from LMDZiso at the NK ice core site since 1958. The *blue lines* show data at Nagarze station, the *red lines* show data at Lhasa station, and the *gray lines* show data from LMDZiso. The *vertical yellow shades* indicate the extreme years based on lowest/highest NK $\delta^{18}O$. On all panels, R (larger than 0.1 are shown only) and slopes show the correlations between NK $\delta^{18}O$ and each climatic parameter

annual layer counting using sub-annually resolved $\delta^{18}O$ and major soluble ions from the 2206 samples, we estimate the age scale uncertainty to be ±1 year from 2006 to 1963 and less than ±2 years prior to 1963 (Zhao et al. 2012).

From low-resolution measurements of $\delta^{18}O$ and $\delta D$ (220 merged samples), Zhao et al. (2012) observed an increasing trend of deuterium excess. They attributed this signal to a decrease of Indian monsoon precipitation on the southern TP through the reduced fraction of annual mean accumulation provided by summer precipitation (associated with a low deuterium excess, Zhao et al. 2012). Here, we expand the investigation of the NK water stable isotope record through our new high-resolution $\delta^{18}O$ data.

This new record will be compared in the next section with local and regional meteorological data. For this purpose, surface air temperature data are available from Lhasa and Nagarze meteorological stations (National Meteorological Information Center of the China Meteorological Administration). We also use 2.5° × 2.5° regional monthly precipitation amount data spanning 1979–2006 from the GPCP (Global Precipitation Climatology Project) (http://www.esrl.noaa.gov/psd/data/gridded/data.gpcp.html). Finally, we also use monthly regional surface air temperature and vertical winds data for the period of interest from NCEP reanalysis data (http://www.esrl.noaa.gov/psd/data/reanalysis/reanalysis.shtml).

To explore the impacts of El Nino/Southern Oscillation (ENSO) on NK $\delta^{18}O$, we use the Nino 3.4 sea surface temperature (SST) index derived from the HadISST1 data set (Rayner et al. 2003) for the period 1870–2006. The relationships between our NK $\delta^{18}O$ and Pacific Decadal Oscillation for the period of 1900–2006 (PDO, http://jisao.washington.edu/pdo/PDO.latest, Zhang et al. 1997; Mantua et al. 1997) as well as Zonal index (defined by the normalized difference in zonal-averaged sea level pressure anomalies between 35 N and 65 N, representing the overall intensity of the surface westerly anomalies over middle latitudes) for the period 1864–2006 (http://ljp.lasg.ac.cn/dct/page/65592, Li and Wang 2003) are also analyzed.

LMDZiso is an atmospheric general circulation model which explicitly includes water stable isotopes (Risi et al. 2010). It captures the seasonal and intra-seasonal variability of TP precipitation $\delta^{18}O$ (Gao et al. 2011; Yao et al. 2012; Gao et al. 2013), but with a cold and dry bias in the southern TP (Gao et al. 2011). Here, we use the inter-annual precipitation and vapor $\delta^{18}O$ outputs from a simulation performed at 2.5° × 3.75° resolution, run from 1958 to 2006 in a "nudged" mode. The Atmospheric Model Intercomparison Project (AMIP) protocol (Gates 1992) is used to prescribe monthly sea surface boundary conditions. The European Centre for Medium-Range Weather Forecasts (ECMWF) reanalysis results (Uppala et al. 2005) are used to nudge the horizontal wind fields with a relaxation time of 1 h. This warrants that the large-scale LMDZiso simulated wind fields are consistent with the observations, and allows to use of the LMDZiso framework to understand and quantify the role of changes in atmospheric circulation in the observed $\delta^{18}O$ variability. A zoomed simulation using the zoom functionality of the LMDZ model, stretching the grid to the horizontal resolution of 50–60 km between 0° and 55°N and 60° and 130°E, are also used here to detect the inter-annual variability.

## 3 Results and discussion

### 3.1 Ice core $\delta^{18}O$ variation

The NK $\delta^{18}O$ record shows large seasonal variations, from −7.0 ‰ at 24.19 m depth to −24.7 ‰ at 16.27 m depth (not shown), with an annual mean value of −16.9 ± 1.7 ‰ from 1864 to 2006 (Fig. 2c). This record contains remarkable multi-decadal variations. Utilizing the regime shift detection algorithm of Rodionov (2004), six different regimes are identified with the regime shift years of 1911, 1921, 1957, 1973 and 1980. High and stable $\delta^{18}O$ values are observed in the nineteenth century, above present-day levels. Two subsequent periods are marked by high $\delta^{18}O$, from the 1910 to 1920 and from 1958 to 1972, with lower values in-between. Since the 1980, NK $\delta^{18}O$ has increased at a mean pace of 0.05 ‰ per year. A sharp decrease occurs from the 1973 to 1978, with the strongest annual $\delta^{18}O$ minimum recorded in 1978. We have investigated whether similar anomalous low $\delta^{18}O$ values are recorded in other Tibetan ice cores. A small minimum is recorded in 1978 in the Malan, Puruogangri and Dasuopu ice cores, and in 1976–1977 in the Guliya, Geladaidong and Tanggula ice cores (not shown). Because the dating uncertainties of these ice cores are usually around ±1 year (Hou et al. 2003; Yao et al. 2006a, b; Joswiak et al. 2010; Kang et al. 2007a; Yao et al. 1997; Wang et al. 2006), we conclude that there is a widespread negative $\delta^{18}O$ anomaly in late 1970s in the Tibetan ice cores, most strongly expressed in NK and Tanggula ice cores.

### 3.2 Relationships with regional meteorological data

These results motivate further exploration of the climatic controls on NK $\delta^{18}O$, with a focus on the period from 1960 to 2006, where the age scale is well established. We first investigate statistical relationship of NK $\delta^{18}O$ with regional meteorological data. Since more than 80 % of precipitation occurs in JJAS, we focus on the relationships between JJAS temperature and precipitation amount and NK $\delta^{18}O$. Since the 1960s, NK $\delta^{18}O$ shows decadal variations which parallel those recorded in Nagarze and Lhasa JJAS temperature.

Without detrending, NK $\delta^{18}O$ inter-annual variations are significantly correlated with Nagarze JJAS temperature ($R = 0.39$, $p < 0.05$, Fig. 2), but not with precipitation. With detrending, NK $\delta^{18}O$ inter-annual variations are still significantly correlated with Nagarze JJAS temperature ($R = 0.47$, $p < 0.01$), but neither with Nagarze precipitation nor with Lhasa temperature and precipitation. Using NCEP gridded JJAS temperature data, we detect significant positive correlations between NK $\delta^{18}O$ and temperature in the central-northern TP and central India, with correlation coefficients <0.6 (Fig. 3a). Using GPCP gridded precipitation data, we identify a weak but significant anti-correlation between NK $\delta^{18}O$ and JJAS precipitation in South East TP (95°–100°E and 25°–30°N, $R > -0.4$, $p < 0.01$), and a positive correlation with JJAS precipitation in the Bay of Bengal (65°–95°E and 10°–20°N, $R < 0.6$, $p < 0.01$, Fig. 3b).

### 3.3 Comparison with LMDZiso simulations and large scale climate fields

We now compare these data with LMDZiso outputs. The simulated temperature is in better agreement with the observed temperature at Nagarze station than that at Lhasa (Fig. 2e, f), especially for the cool periods (1968, 1977–1979, 1992–1997). However, the model overestimates the variability of precipitation amount, compared with observations at Lhasa and Nagarze stations (Fig. 2g, h), especially before 1980s. We observe a better model-data agreement between NK $\delta^{18}O$ and the simulated water vapor $\delta^{18}O$ than with the simulated precipitation $\delta^{18}O$ for the period of 1958–2006 (Fig. 2a–c); this could be related to the intermittency of precipitation, or to post-deposition processes (Steen-Larsen et al. 2014).

Some inter-annual changes in the simulated annual temperature, precipitation amount and water vapor $\delta^{18}O$ coincide with changes recorded in NK $\delta^{18}O$ (Fig. 2a–c, f, h). Within LMDZiso, the percentage of the simulated precipitation $\delta^{18}O$ which can be explained by a linear correlation with local simulated temperature and precipitation is weak and can only explain less than 10 % of precipitation $\delta^{18}O$ variance (Fig. 2b, f, h), even when considering a multiple regression that includes the temperature and precipitation amount together. The lowest NK $\delta^{18}O$ is observed and simulated in 1978, and it is associated with the most negative anomalies of simulated annual temperature (Fig. 2e), precipitation amount (Fig. 2h) and vapor $\delta^{18}O$ (Fig. 2a).

NK $\delta^{18}O$ is weakly positively correlated with JJAS simulated precipitation amount in the tropical Indian Ocean ($R < 0.6$, $p < 0.1$) and, as in GPCP, anti-correlated with LMDZiso precipitation in the southeast TP ($R > -0.3$, $p < 0.1$) (Fig. 3c). NK $\delta^{18}O$ is most strongly correlated with vapor $\delta^{18}O$ at 425 hPa for the period of 1979–2006 (pressure level closest to NK ice core drilling site elevation) in the tropical Indian Ocean (10°S–10°N, 85°E–130°E) and the west Pacific Ocean (Fig. 3d). In addition, NK $\delta^{18}O$ is significantly positive correlated with JJAS zonal wind (U wind) at 500 hPa in 32°N–40°N and 50°E–80°E from 1979 to 2006 (Fig. 3e). Meanwhile, NK $\delta^{18}O$ is significantly negatively correlated with JJAS U wind at 500 hPa over the tropical Indo-Pacific Ocean during the same period (Fig. 3e). After 1979, the significant positive correlation between NK $\delta^{18}O$ and meridional wind (V wind) exists in northwest TP (Fig. 3f). NK $\delta^{18}O$ is also significantly positively correlated with the observed SST since 1982 in the tropical Indo-Pacific Ocean (between 5°N and 20°S, Fig. 3i). In winter, the significantly positive correlation only exists in 0°–10°N and 95°E–120°E with U wind, and the Persian Gulf as well as a small part of Arabian Sea with V wind (Fig. 3f, h). NK $\delta^{18}O$ show significantly positive correlation with winter SST in the western and northern Arabian Sea and the Philippines (Fig. 3j).

These statistical analyses suggest large-scale atmospheric circulation drivers of NK $\delta^{18}O$ inter-annual variability. The mechanisms relating large-scale atmospheric circulation and tropical precipitation isotopic composition are complex, and have been explored in atmospheric models. Following earlier works of Hoffmann (2003) and Vuille et al. (2003) for the Andes, Brown et al. (2006) identified strong imprints of monsoons, meridional migration of the ITCZ and ENSO in tropical precipitation isotopic composition, through processes affecting rainout intensity and convection height. Other ice cores in the central TP, Arctic, Antarctic, and subpolar regions were also interpreted to depict rapid changes in atmospheric circulation after the mid-1970s (Kang et al. 2002; Kaspari et al. 2007; Schneider et al. 2012; Kelsey et al. 2012).

The statistical analyses show that local temperature or precipitation account for less than 50 % of NK $\delta^{18}O$ variability in both observations and LMDZiso, and point to processes associated with moisture transport and large-scale atmospheric circulation, at the inter-annual scale. At the intra-summer scale, different controls were identified for Lhasa precipitation $\delta^{18}O$ variability (Gao et al. 2013). Combining daily precipitation isotopic composition measurements and satellite information on convection and water vapor isotopic composition, He et al. (2015) showed a dominant control through convective activity above North India: enhanced convection (and increased precipitation above N. India) depletes surface water $\delta^{18}O$, and this depletion is further amplified along the orographic uplift of moister air, and finally by enhanced subsidence of depleted vapor towards Lhasa. Our study suggests that controls at the intra-seasonal time scale cannot be extrapolated at the inter-annual scale. Indeed, the statistical analyses show that, at the inter-annual scale, enhanced JJAS precipitation above the southern Bay of Bengal and enriched vapor $\delta^{18}O$

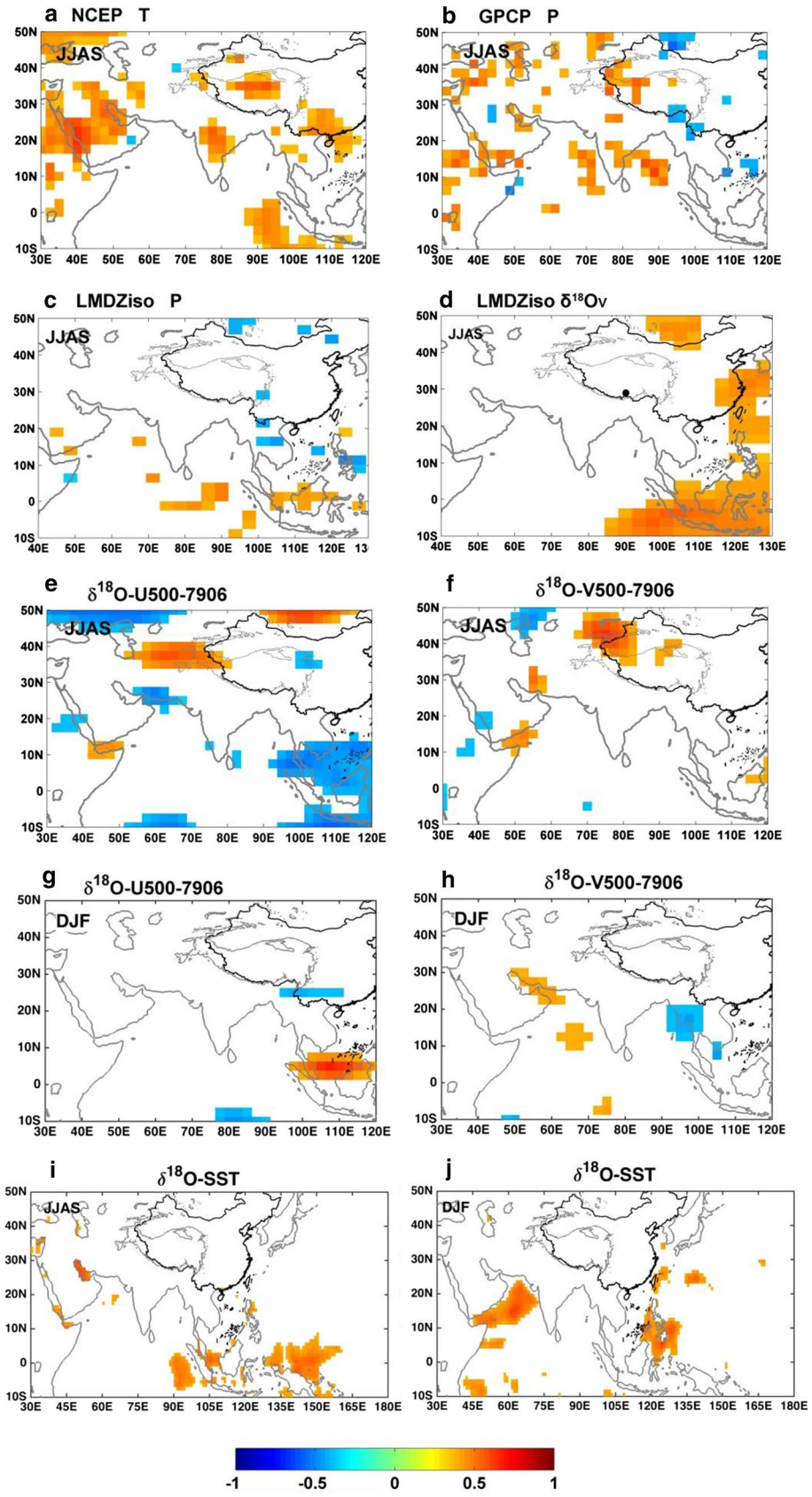


**Fig. 3** Spatial distribution of linear correlation coefficients between NK ice core $\delta^{18}O$ and regional air temperature and precipitation from observations and LMDZiso simulations, as well as winds and SST. **a** NCEP gridded JJAS surface air temperature data (1948–2006), **b** GPCP gridded JJAS precipitation data (1979–2006), **c** JJAS precipitation amount simulated from LMDZiso (1979–2006). **d** Correlation coefficients between NK ice core $\delta^{18}O$ and LMDZiso JJAS vapor $\delta^{18}O$ at 425 hPa hight (1979–2006). **e** Correlation coefficients between NK ice core $\delta^{18}O$ and NCEP gridded JJAS zonal wind (U wind) at 500 hPa height (1979–2006). **f** Correlation coefficients between NK ice core $\delta^{18}O$ and NCEP gridded JJAS meridional wind (V wind) at 500 hPa height (1979–2006). **g** Correlation coefficients between NK ice core $\delta^{18}O$ and NCEP gridded DJF zonal wind at 500 hPa height (1979–2006). **h** Correlation coefficients between NK ice core $\delta^{18}O$ and NCEP gridded DJF meridional wind at 500 hPa height (1979–2006). **i** Correlation coefficients between NK ice core $\delta^{18}O$ and NCEP gridded JJAS SST (1982–2006). **j** Correlation coefficients between NK ice core $\delta^{18}O$ and NCEP gridded DJF SST (1982–2006). On all maps, only correlations significant at the 95 % confidence level are shown

in the tropical ocean and west Pacific Ocean at 425 hPa level are consistent with an $\delta^{18}O$ enrichment at NK high elevation site, responding to a common large-scale mode of variability.

We now discuss the mechanisms which may affect the recent NK $\delta^{18}O$ trend, since 1980. While warming is expected to induce enrichment in the NK $\delta^{18}O$, one process is expected to compensate for temperature effects and weaken the NK $\delta^{18}O$ increase after 1980. Enhanced westerlies (Yuan et al. 2014), accounting for a larger proportion of annual precipitation, also provide depleted moisture though long distance transport.

### 3.4 Causes of the late 1970s NK $\delta^{18}O$ shift: statistical analysis

In order to further explore the processes controlling interannual variations of NK $\delta^{18}O$, we focus on the sharp decrease observed in the late 1970s (Fig. 2c). Meteorological data show cold conditions in 1978 at both stations (Fig. 2e) as well as in the central TP (Kang et al. 2007b), with the coldest summer encountered in 1976 at Nagarze and Lhasa (Fig. 2d).

During the mid-1970s, shifts in North Pacific climate regime were associated with a deepening of the Aleutian Low and a strengthening of the mid-latitude westerlies (Miller et al. 1994; Nakamura et al. 1997; Mantua et al. 1997; Zhang et al. 1997; Wu et al. 2005), which affected Indian monsoon strength (Trenberth and Hurrell 1994; Wang and Ding 2006). This regime shift also involved changes in the PDO and ENSO (Guilderson and Schrag 1998; Mantua and Hare 2002; Alexander et al. 2002). The ENSO influence on TP moisture and ice core $\delta^{18}O$ are also found at Dasuopu (Brown et al. 2006) and other tropical ice cores (Vuille et al. 2003; Hoffmann 2003a; Bradley et al. 2003). This motivates an investigation of the relationships between NK $\delta^{18}O$ and Pacific modes of variability.

The spectral analysis of NK $\delta^{18}O$, performed with a wavelet and Multi-Taper method (not shown) reveals a significant periodicity at 2.7 years, also suggesting an ENSO influence on NK $\delta^{18}O$. During several intervals, NK $\delta^{18}O$ is significantly correlated with Nino 3.4 SST index for different seasons. During the cold PDO phase of 1943–1976 (Fig. 4e), NK $\delta^{18}O$ is positively correlated with December-February (DJF) Nino 3.4 SST anomalies ($R = 0.32$, $p = 0.06$ and up to 0.44, $p = 0.01$ when excluding 1973, Fig. 4a, b). Since 1980, during the warm phase of PDO, NK $\delta^{18}O$ is anti-correlated with May–September (MJJAS) Nino 3.4 SST anomalies ($R = -0.32$, $p = 0.11$ and up to $R = -0.45$, $p = 0.02$ excluding 1984) (Fig. 4a, c, e). The NK $\delta^{18}O$ minimum at the end of the 1970s coincides with a PDO phase shift (from negative phase to positive phase, Grigholm et al. 2009), an inflexion point of the zonal index (onset of a fast increase, Fig. 4a, d) as well as ENSO

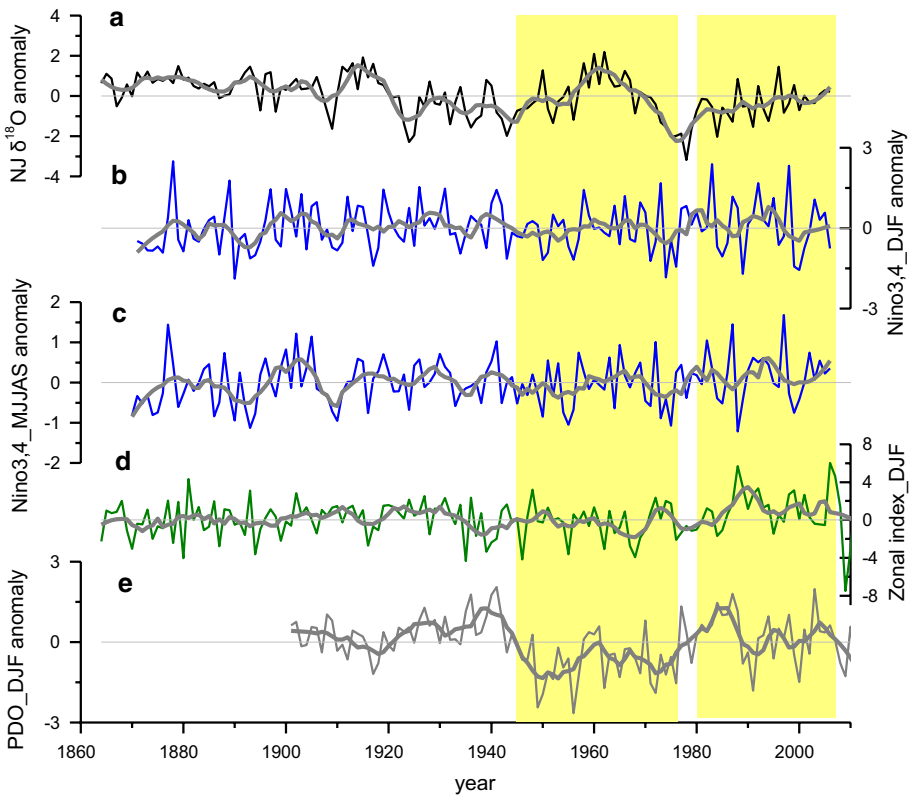


**Fig. 4** Comparison of (*a*) the NK $\delta^{18}O$ anomalies, (*b*) December–February Nino 3.4 SST anomalies from 1870 to 2006, (*c*) May–September Nino 3.4 SST anomalies from 1870 to 2006 and (*d*) Zonal index from 1864 to 2006 as well as (*e*) December–February PDO from 1900 to 2006. *Thin lines* show annual data and *thick lines* show 10-year smoothing. *Horizontal gray lines* depict zero levels

(increase in frequency and intensity). This again indicates that the most remarkable NK $\delta^{18}O$ negative anomaly is associated with changes of the large-scale atmospheric circulations, although a partial role of temperature cannot be excluded.

The mechanism by which the PDO/ENSO could affect the southern TP ice core $\delta^{18}O$ was hypothesized through the Indian monsoon and westerlies changes. An "atmospheric bridge" connects the ENSO/PDO-driven large-scale atmospheric circulation changes with the SST, wind, and humidity from the North Pacific to Indian Oceans (Alexander et al. 2002), which then alter the strength and intensity of the Indian monsoon. In the decade prior to the climate shift, SST changed in the western subtropical Pacific, leading to a shift of atmospheric circulation and changes of SST in other parts of Pacific, then driving ENSO variability by modulating the trade winds (Barnett et al. 1999; Vimont et al. 2001, 2003; Alexander et al. 2002). After 1976, the cooling of SST of central Pacific and subtropics associated with central Pacific El Niño forced changes in the extra-tropical atmospheric circulation (Lorenzo et al. 2010), and surface wind anomalies switched from easterly to westerly. In return, tropical SST changes associated with the recurrence of El Niño from the mid 1970s to the late 1980s reinforced north Pacific changes and westerly wind anomalies (Wu et al. 2005). The warm phase of PDO during the boreal winter season affects subtropical and tropical SST persisting into the next monsoon season (Krishnamurthy and Krishnamurthy 2013). This pattern explains the anti-correlation between NK $\delta^{18}O$ and May–September (MJJAS) Nino 3.4 SST anomalies since 1980. They drive changes in equatorial trade winds that reinforce the equatorial Walker circulation and lead to enhanced ascending motion in the central Pacific and the equatorial Indian Ocean, weakening the Indian monsoon (Krishnamurthy and Krishnamurthy 2013).

With the increase of SST and zonal wind in the tropical Indo-Pacific Ocean, the evaporation of surface ocean water strengthens, providing local vapor which is not depleted in $\delta^{18}O$. The increased local evaporation replenishes the monsoon flow and may explain the reduced depletion of NK $\delta^{18}O$. In the southern TP, these processes can be compensated by the fact that a weaker Indian monsoon also leads to an increase in moisture transported from western remote sources (e.g. Persian Gulf), which is characterized by low $\delta^{18}O$. El Niño events further reduce the strength of Indian monsoon through the descending Hadley branch, while the situation is more ambiguous during La Niña events (Mantua and Hare 2002; Krishnamurthy and Krishnamurthy 2013; Sano et al. 2013; Miyasaka et al. 2014). The transport of vapor over the tropical Indo-Pacific Ocean changes with winds corresponding to the PDO/ENSO phase. In El Nino winter, the westerlies decreases due to the warmer SST in tropical Indian Ocean, resulting in more water vapor transport to north; after 1980, during the warm phase of PDO, cyclones prevail in the west of Philippines in La Nina winter, helping stronger moisture transport from Indian Ocean to continent; before 1980, the condition is opposite (Yuan et al. 2014). The influences of El Nino/La Nina on anticyclone/cyclone close to the Philippines however are inconsistent and asymmetric (Wu et al. 2010). Meanwhile, the deepening of the Aleutian Low and strengthening of the winter mid-latitude westerlies are associated with colder conditions (Miller et al. 1994; Alexander et al. 2002; Mantua and Hare 2002), further depleting precipitation $\delta^{18}O$.

### 3.5 Causes of the late 1970s NK $\delta^{18}O$ shift: analysis using LMDZiso

The role of large-scale circulation is now explored using LMDZiso JJAS precipitation $\delta^{18}O$. The model simulates too enriched precipitation $\delta^{18}O$, a feature common to other atmospheric models (Yao et al. 2013), but also underestimates the magnitude of inter-annual $\delta^{18}O$ variations, and does not produce decadal variability. We note that the model caveats could be linked to the atmospheric model resolution, as it cannot resolve small-scale topographic features which may play a key role on the inter-annual variability of high elevation precipitation $\delta^{18}O$ (Gao et al. 2011). The zoomed simulation obviously improves the intra-annual precipitation $\delta^{18}O$, but not its inter-annual variability. We also stress the fact that the ice core record can be associated with a noticeable noise level, due to post deposition processes such as wind scouring, and does include a signal from the non-monsoon season. However, LMDZiso does produce a sharp decrease in NK precipitation $\delta^{18}O$ in the late 1970s, and minimum values in 1978. We therefore use the framework provided by the LMDZiso simulation to understand the processes controlling the JJAS $\delta^{18}O$ depletion in 1978–1979, compared to 1982–1983 levels (Fig. 5). The associated precipitation $\delta^{18}O$ anomaly has a magnitude of ~1.5 ‰ (Fig. 5a), extends over all the TP and is also depicted in the vapor $\delta^{18}O$ (~1.7 ‰, Fig. 5c).

We use a decomposition of the associated $\delta^{18}O$ anomaly into several terms, which account for the effects of rain-vapor disequilibrium, fractionation coefficients, local temperature, temperature at the source, local relative humidity, and residual effects including convection and large-scale transport (See Appendix in Supplementary Material). This approach shows a key role of changes in the intensity of Rayleigh distillation due to changes in temperature. In 1978–1979, LMDZ simulates TP regional cooling, consistent with meteorological data, which explains a depletion of about 0.7 ‰. Residual effects including large-scale transport however account for an additional depletion of about 1 ‰.

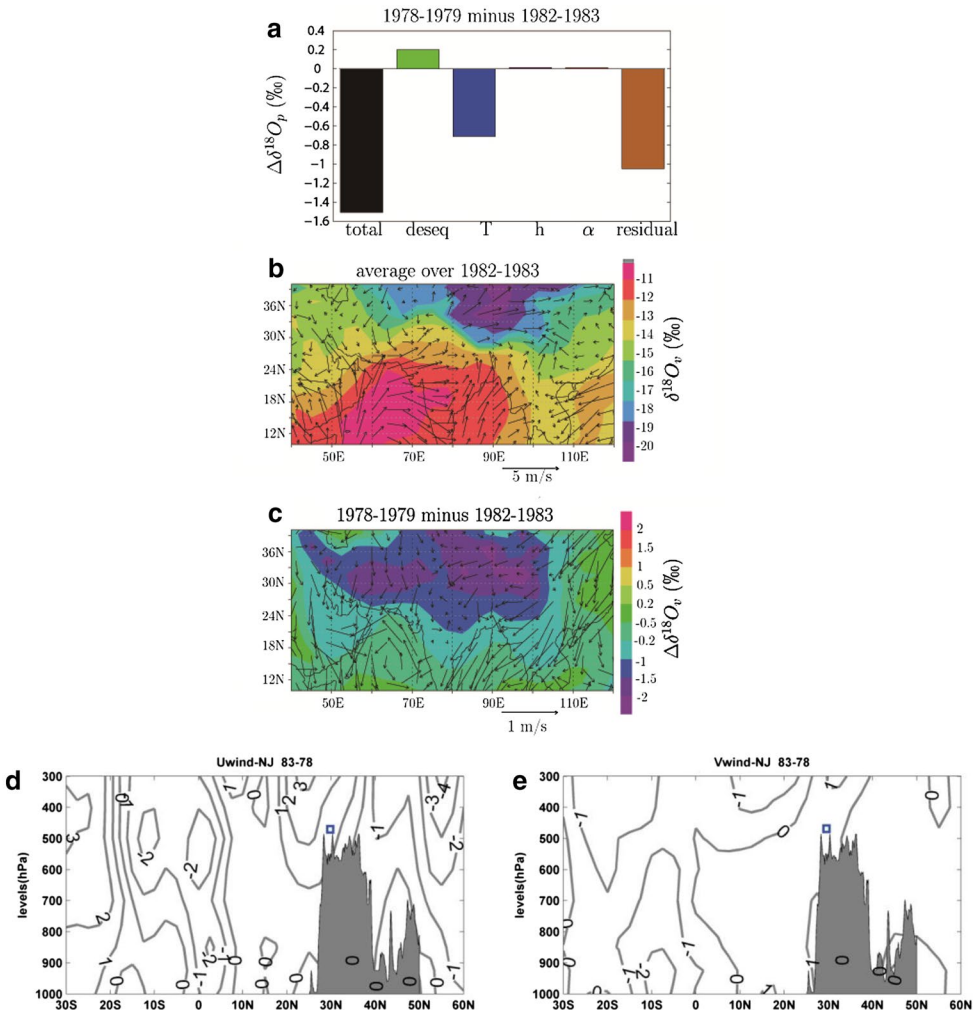


**Fig. 5** Attribution of the precipitation $\delta^{18}O$ anomaly from 1978–1979 to 1982–1983 using the LMDZiso model. **a** Decomposition of the precipitation $\delta^{18}O$ anomaly into a sum of five contributions due to rain-vapor disequilibrium (deseq), fractionation coefficients (α), temperature (T), local relative humidity (h), and residual effects (residual) including convection and large-scale transport (see Appendix in Supplementary Material). **b** Map showing the 1982–1983 pattern of JJAS vapor $\delta^{18}O$ at the lowest atmospheric model level (*colors*) and pattern of JJAS winds at the lowest atmospheric level (*vectors*). **c** Same as (**b**) but for the difference between 1982 and 1983 and 1978–1979. Vertical profiles of difference between 1983 and 1978 for zonal (**d**) and meridional (**e**) winds along 90°E longitude from 30°S to 60°N, from NCEP reanalyses, downloaded from http://www.esrl.noaa.gov/psd/data/gridded/data.ncep.reanalysis.derived.pressure.html. The *grey shading* depicts the TP topography. The *blue square* shows the location of NK ice core

The pattern of changes in atmospheric circulation (Fig. 5c) depicts a reduced northward monsoon flow, and a large North-Easterly anomaly of −0.5 m/s (Fig. 5b, c). Combined with the average JJAS vapor $\delta^{18}O$ South West-North East gradient of about $-2.4 \times 10^{-3}$ ‰ per km (Fig. 5b) and a residence time of water vapor of about 10 days, this anomalous circulation pattern can account for the residual anomaly of low-level water vapor $\delta^{18}O$ anomaly of ~−1 ‰. The precipitation $\delta^{18}O$ composition then follows tightly that of the low-level water vapor, variations in precipitation-vapor differences accounting for less than 0.2 ‰ of precipitation variations.

The large-scale circulation effects are clearly visible in the latitudinal and vertical structure of JJAS zonal and meridional winds from NCEP reanalyses along a transect at 90°E for 1978 and 1983 (Fig. 5d, e). Regarding westerly wind (U, Fig. 5d), the data depict a decrease of low level winds (<500 hPa) at 0°–20°N, and an increase of high level winds (500 hPa) at 20°N–30°N in 1983 compared to 1978. The meridional profile displays a decrease of the low atmosphere southerly winds in 1983 compared to 1978 (Fig. 5e). This illustrates the decrease of Indian monsoon and increase of westerlies in 1983 compared to 1978, consistent with the statistical analysis and the tele-connections evidenced in Sect. 3.4.

In summary, the abrupt depletion of NK $\delta^{18}O$ in 1978 is captured by the LMDZiso simulation. It is mostly attributed to a depletion of water vapor $\delta^{18}O$ due to the change in temperature and in large-scale atmospheric circulation. The effect of large-scale atmospheric circulation on vapor $\delta^{18}O$ is found to be larger than that of temperature.

## 4 Conclusions and perspectives

In this manuscript, we have reported the $\delta^{18}O$ signal recorded by a new Southern Tibetan ice core. In contrast with earlier studies, our record does not show unprecedented warming during the last decades. It is dominated by decadal variations, including a remarkable isotopic depletion during the late 1970s. Statistical analyses stress a significant anti-correlation with precipitation amount

($p < 0.05$) in the surrounding areas, as well as zonal wind at 500 hPa in the tropical Indo-Pacific oceans, and a positive correlation with precipitation amount in the Bay of Bengal, as well as with surface temperature in TP, India and summer tropical SSTs. Significant relationships are detected with large-scale modes of variability (ENSO and PDO). The importance of large-scale atmospheric circulation is further supported by the ability of the atmospheric general circulation model LMDZiso to resolve the 1978 isotopic anomaly. The model shows that this anomaly extends over all of TP, and is positively related to an anomaly in water vapor $\delta^{18}O$ in the tropical Indo-Pacific region. Within the model framework, we isolated the driver of this anomaly, which is mostly due to an abnormal atmospheric circulation, marked by enhanced westerlies, and a reduced monsoon flow, while air temperature also affects this anomaly through changes in Rayleigh distillation, but with a smaller effect than that of circulation alone.

This work demonstrates the ability of TP annual ice core $\delta^{18}O$ to record abrupt shifts in atmospheric circulation and provides a methodology to evaluate the magnitude of local versus large-scale controls on ice core $\delta^{18}O$. This will motivate further integration of high-resolution precipitation $\delta^{18}O$ records from multiple archives (ice cores, but also tree ring cellulose, speleothems and lake sediment records) in order to map the spatial and temporal variability of $\delta^{18}O$, and to characterize past changes in regional atmospheric circulation.

**Acknowledgments** This work was funded by the National Natural Science Foundation of China (Grant Nos. 41471053, 41101061, 41190080 and 41125003), the "Strategic Priority Research Program (B)" of the Chinese Academy of Sciences (Grant No. XDB03030100), and China-France Caiyuanpei Program. We thank the staff which performed the ice core drilling and appreciate the important contribution of Huabiao Zhao, Mo Wang and Chenglong Zhang for ice cutting and dust samples measurements, as well as the support of Dongmei Qu for isotope measurements. We also thank Third Pole Environment Database for some data support (http://www.tpedatabase.cn).



## References

Alexander MA, Blade I, Newman M, Lanzante JR, Lau NC, Scott JD (2002) The atmospheric bridge: the influence of ENSO teleconnections on air–sea interaction over the global oceans. J Clim 15(16):2205–2231

Barnett TP, Pierce DW, Latif M, Dommenget D, Saravanan R (1999) Interdecadal interactions between the tropics and midlatitudes in the Pacific basin. Geophys Res Lett 26:615–618

Bradley RS, Vuille M, Hardy D, Thompson LG (2003) Low latitude ice cores record Pacific sea surface temperatures. Geophys Res Lett 30(4):1174. doi:10.1029/2002GL016546

Breitenbach SFM, Adkins JF, Meyer H, Marwan N, Kumar KK, Haug GH (2010) Strong influence of water vapor source dynamics on stable isotopes in precipitation observed in Southern Meghalaya, NE India. Earth Planet Sci Lett 292(1–2):212–220. doi:10.1016/j.epsl.2010.01.038

Brown J, Simmonds I, Noone D (2006) Modeling delta o-18 in tropical precipitation and the surface ocean for present-day climate. J Geophys Res-Atmos. doi:10.1029/2004jd005611

Gao J, Tian L, Liu Y, Gong T (2009) Oxygen isotope variation in the water cycle of the Yamzho lake Basin in southern Tibetan Plateau. Chin Sci Bull 54(16):2758–2765. doi:10.1007/s11434-009-0487-6

Gao J, Masson-Delmotte V, Yao T, Tian L, Risi C, Hoffmann G (2011) Precipitation water stable isotopes in the south Tibetan Plateau: observations and modeling. J Clim 24(13):3161–3178. doi:10.1175/2010jcli3736.1

Gao J, Masson-Delmotte V, Risi C, He Y and Yao TD (2013) What controls precipitation 18O in the southern Tibetan Plateau at seasonal and intra-seasonal scales? A case study at Lhasa and Nyalam. Tellus B 65(21043). http://dx.doi.org/10.3402/tellusb.v65i0.21043

Gates WL (1992) AMIP: the atmospheric model intercomparison project. Bull Am Meteorol Soc 73(12):1962–1970

Grigholm B, Mayewski PA, Kang S, Zhang Y, Kaspari S, Sneed SB, Zhang Q (2009) Atmospheric soluble dust records from a Tibetan ice core: possible climate proxies and teleconnection with the pacific decadal oscillation. J Geophys Res-Atmos. doi:10.1029/2008jd011242

Guilderson TP, Schrag DP (1998) Abrupt shift in subsurface temperatures in the tropical pacific associated with changes in El Nino. Science 281(5374):240–243. doi:10.1126/science.281.5374.240

He Y et al (2015) Impact of atmospheric convection on south Tibet summer precipitation isotopologue composition using a combination of in situ measurements, satellite data and atmospheric general circulation modeling. J Geophys Res Atmos 120. doi:10.1002/2014JD022180

Hoffmann G (2003) Taking the pulse of the tropical water cycle. Science 301:776. doi:10.1126/science.1085066

Hoffmann G, Ramirez E, Taupin JD, Francou B, Ribstein P, Delmas R, Durr H, Gallaire R, Simoes J, Schotterer U, Stievenard M, Werner M (2003) Coherent isotope history of andean ice cores over the last century. Geophys Res Lett. doi:10.1029/2002gl014870

Hou S, Qin D, Zhang D, Kang S, Mayewski PA, Wake CP (2003) A 154a high-resolution ammonium record from the Rongbuk Glacier, north slope of Mt. Qomolangma (Everest), Tibet-Himal region. Atmos Environ 37(5):721–729. doi:10.1016/S1352-2310(02)00582-4

Johnson KR, Ingram BL (2004) Spatial and temporal variability in the stable isotope systematics of modern precipitation in china: implications for paleoclimate reconstructions. Earth Planet Sci Lett 220(3–4):365–377. doi:10.1016/s0012-821x(04)00036-6

Joswiak DR, Yao T, Wu G, Xu B, Zheng W (2010) A 70-yr record of oxygen-18 variability in an ice core from the Tanggula Mountains, central Tibetan Plateau. Clim Past 6(2):219–227

Kang S, Mayewski PA, Qin D, Yan Y, Hou S, Zhang D, Ren J, Kruetz K (2002) Glaciochemical records from a Mt. Everest ice core: relationship to atmospheric circulation over Asia. Atmos Environ 36(21):3351–3361. doi:10.1016/s1352-2310(02)00325-4

Kang S, Zhang Y, Qin D, Ren J, Zhang Q, Grigholm B, Mayewski PA (2007a) Recent temperature increase recorded in an ice core in the source region of Yangtze River. Chin Sci Bull 52(6):825–831. doi:10.1007/s11434-007-0140-1

Kang S, Qin D, Ren J, Zhang Y, Kaspari S, Mayewski PA, Hou S (2007b) Annual accumulation in the Mt. Nyainqentanglha ice core, southern Tibetan Plateau, China: relationships to atmospheric circulation over Asia. Arct Antarct Alp Res 39(4):663–670

Kaspari S, Mayewski P, Kang S, Sneed S, Hou S, Hooke R, Kreutz K, Introne D, Handley M, Maasch K, Qin D, Ren J (2007) Reduction in northward incursions of the South Asian monsoon since approximate to 1400 ad inferred from a Mt. Everest ice core. Geophys Res Lett. doi:10.1029/2007gl030440

Kelsey EP, Wake CP, Yalcin K, Kreutz K (2012) Eclipse ice core accumulation and stable isotope variability as an indicator of North Pacific climate. J Clim 25(18):6426–6440

Kreutz KJ, Mayewski PA, Pittalwala II, Meeker LD, Twickler MS, Whitlow SI (2000) Sea level pressure variability in the Amundsen Sea region inferred from a West Antarctic glaciochemical record. J Geophys Res-Atmos 105(D3):4047–4059. doi:10.1029/1999jd901069

Krishnamurthy L, Krishnamurthy V (2013) Influence of PDO on South Asian summer monsoon and monsoon–ENSO relation. Clim Dyn 42(9–10):2397–2410

Li JP, Wang XLJ (2003) A modified zonal index and its physical sense. Geophys Res Lett. doi:10.1029/2003gl017441

Liu XD, Chen BD (2000) Climatic warming in the Tibetan Plateau during recent decades. Int J Climatol 20(14):1729–1742

Lorenzo DE, Cobb KM, Furtado JC, Schneider N, Anderson BT, Bracco A, Alexander MA, Vimont DJ (2010) Central pacific El Nino and decadal climate change in the North Pacific ocean. Nat Geosci 3(11):762–765. doi:10.1038/ngeo984

Mantua NJ, Hare SR (2002) The Pacific decadal oscillation. J Oceanogr 58:35–44

Mantua NJ, Hare SR, Zhang Y, Wallace JM, Francis RC (1997) A pacific interdecadal climate oscillation with impacts on salmon production. Bull Am Meteorol Soc 78(6):1069–1079

Meeker LD, Mayewski PA (2002) A 1400 year long record of atmospheric circulation over the North Atlantic and Asia. Holocene 12(3):257–266

Miller JA, Cayan DR, Barnett TP et al (1994) The 1976–77 climate shift of the Pacific Ocean. Oceanography 7(1):21–26

Miyasaka T, Nakamura H, Taguchi B, Nonaka M (2014) Multidecadal modulations of the low-frequency climate variability in the wintertime North Pacific since 1950. Geophys Res Lett 41(8):2948–2955

Nakamura H, Lin G, Yamagata T (1997) Decadal climate variability in the North Pacific during the recent decades. Bull Am Meteorol Soc 78(10):2215–2225

Qin D, Mayewski PA, Wake CP et al (2000) Evidence for recent climate change from ice cores in the central Himalayas. Ann Glaciol 31:153–158

Qin J, Yang K, Liang S, Guo X (2009) The altitudinal dependence of recent rapid warming over the Tibetan Plateau. Clim Change 97(1–2):321–327. doi:10.1007/s10584-009-9733-9

Rayner NA, Parker DE, Horton EB, Folland CK, Alexander LV, Rowell DP, Kent EC, Kaplan A (2003) Global analyses of sea surface temperature, sea ice, and night marine air temperature since the late nineteenth century. J Geophys Res-Atmos. doi:10.1029/2002jd002670

Risi C, Bony S, Vimeux F, Jouzel J (2010) Water-stable isotopes in the LMDZ4 general circulation model: model evaluation for present-day and past climates and applications to climatic interpretations of tropical isotopic records. J Geophys Res-Atmos 115(d24123). doi:10.1029/2010jd015242

Rodionov SN (2004) A sequential algorithm for testing climate regime shifts. Grophys Res Lett. doi:10.1029/2004GL019448

Sano M, Tshering P, Komori J, Fujita K, Xu C, Nakatsuka T (2013) May–september precipitation in the Bhutan Himalaya since 1743 as reconstructed from tree ring cellulose o-18. J Geophys Res-Atmos 118(15):8399–8410. doi:10.1002/jgrd.50664

Schneider DP, Okumura Y, Deser C (2012) Observed Antarctic interannual climate variability and tropical linkages. J Clim 25(12):4048–4066

Steen-Larsen HC, Masson-Delmotte V, Hirabayashi M, Winkler R, Satow K, Prie F, Bayou N, Brun E, Cuffey KM, Dahl-Jensen D, Dumont M, Guillevic M, Kipfstuhl S, Landais A, Popp T, Risi C, Steffen K, Stenni B, Sveinbjornsdottir AE (2014) What controls the isotopic composition of Greenland surface snow? Clim Past 10(1):377–392. doi:10.5194/cp-10-377-2014

Thompson LG, Yao T, Mosley-Thompson E, Davis ME, Henderson KA, Lin PN (2000) A high-resolution millennial record of the South Asian monsoon from Himalayan ice cores. Science 289(5486):1916–1919. doi:10.1126/science.289.5486.1916

Tian L, Masson-Delmotte V, Stievenard M, Yao T, Jouzel J (2001) Tibetan Plateau summer monsoon northward extent revealed by measurements of water stable isotopes. J Geophys Res-Atmos 106(D22):28081–28088. doi:10.1029/2001jd900186

Tian L, Yao T, Schuster PF, White JWC, Ichiyanagi K, Pendall E, Pu J, Wu Y (2003) Oxygen-18 concentrations in recent precipitation and ice cores on the Tibetan Plateau. J Geophys Res-Atmos. doi:10.1029/2002jd002173

Tian L, Yao T, Yu W et al (2006) Stable isotopes of precipitation and ice core on the Tibetan Plateau and moisture transports. Quat Sci 26(2):145–152

Trenberth KE, Hurrell JW (1994) Decadal atmosphere-ocean variations in the Pacific. Clim Dyn 9(6):303–319

Uppala SM et al (2005) The ERA-40 re-analysis. Q J R Meteorol Soc 131(612):2961–3012

Vimont DJ, Battisti DS, Hirst AC (2001) Footprinting: a seasonal connection between the tropics and mid-latitudes. Geophys Res Lett 28(20):3923–3926. doi:10.1029/2001gl013435

Vimont DJ, Wallace JM, Battisti DS (2003) The seasonal footprinting mechanism in the pacific: implications for ENSO. J Clim 16(16):2668–2675

Vuille M, Bradley RS, Werner M, Healy R, Keimig F (2003) Modeling $\delta^{18}O$ in precipitation over the tropical Americas, part I, interannual variability and climatic controls. J Geophys Res 108 doi:10.1029/2001JD002038

Vuille M, Werner M, Bradley RS, Keimig F (2005) Stable isotopes in precipitation in the Asian monsoon region. J Geophys Res-Atmos. doi:10.1029/2005jd006022

Wang B, Ding QH (2006) Changes in global monsoon precipitation over the past 56 years. Geophys Res Lett. doi:10.1029/2005gl025347

Wang N, Yao T, Pu J, Zhang Y, Sun W (2006) Climatic and environmental changes over the last millennium recorded in the Malan ice core from the northern Tibetan Plateau. Sci China Ser D 49(10):1079–1089. doi:10.1007/s11430-006-1079-9

Wang B, Bao Q, Hoskins B, Wu G, Liu Y (2008) Tibetan Plateau warming and precipitation changes in East Asia. Geophys Res Lett. doi:10.1029/2008gl034330

Wu LX, Lee DE, Liu ZY (2005) The 1976/77 north pacific climate regime shift: the role of subtropical ocean adjustment and coupled ocean-atmosphere feedbacks. J Clim 18(23):5125–5140. doi:10.1175/jcli3583.1

Wu B, Li T, Zhou TJ (2010) Asymmetry of atmospheric circulation anomalies over the western North Pacific between El Niño and La Nia. J Clim 23(18):4807–4822

Xiao C, Mayewski PA, Qin D et al (2004) Sea level pressure variability over the southern Indian Ocean inferred from a glacioc hemical record in Princess Elizabeth Land, East Antarctica. J Geophys Res 109(DI6):DI6101. doi:10.1029/2003JD004065

Yao T, Shi Y, Thompson LG (1997) High resolution record of paleoclimate since the Little Ice Age from the Tibetan ice cores. Quatern Int 37:19–23. doi:10.1016/1040-6182(96)00006-7

Yao TD, Guo XJ, Thompson L, Duan KQ, Wang NL, Pu JC, Xu BQ, Yang XX, Sun WZ (2006a) Delta o-18 record and temperature change over the past 100 years in ice cores on the Tibetan Plateau. Sci China Ser D-Earth Sci 49(1):1–9. doi:10.1007/s11430-004-5096-2

Yao TD, Li ZX, Thompson LG, Thompson EM, Wang YQ, Tian L, Wang NL, Duan KQ (2006b) $\delta^{18}O$ records from Tibetan ice cores reveal differences in climatic changes. Ann Glaciol 43(1):1–7. doi:10.3189/172756406781812131

Yao T, Thompson L, Yang W, Yu W, Gao Y, Guo X, Yang X, Duan K, Zhao H, Xu B, Pu J, Lu A, Xiang Y, Kattel DB, Joswiak D (2012) Different glacier status with atmospheric circulations in Tibetan Plateau and surroundings. Nat Clim Change 2(9):663–667. doi:10.1038/nclimate1580

Yao T, Masson-Delmotte V, Gao J, Yu W, Yang X, Risi C, Sturm C, Werner M, Zhao H, He Y, Ren W, Tian L, Shi C, Hou S (2013) A review of climatic controls on delta o-18 in precipitation over the Tibetan Plateau: observations and simulations. Rev Geophys. doi:10.1002/rog.20023

Yuan Y, Li C, Yang S (2014) Decadal anomalies of winter precipitation over southern China in association with El Niño and La Niña. Acta Meteorol Sin 72(2):237–255

Zhang Y, Wallace JM, Battisti DS (1997) ENSO-like interdecadal variability: 1900–1993. J Clim 10:1004–1020

Zhao H, Xu B, Yao T, Wu G, Lin S, Gao J, Wang M (2012) Deuterium excess record in a southern Tibetan ice core and its potential climatic implications. Clim Dyn 38(9–10):1791–1803. doi:10.1007/s00382-011-1161-7